Multiobjectivization for Parameter Estimation: a Case-Study on the Segment Polarity Network of Drosophila

Tim Hohm
Computer Engineering and Networks Laboratory
ETH Zurich
8092 Zurich, Switzerland
tim.hohm@tik.ee.ethz.ch

Eckart Zitzler
Computer Engineering and Networks Laboratory
ETH Zurich
8092 Zurich, Switzerland
eckart.zitzler@tik.ee.ethz.ch

ABSTRACT

Mathematical modeling for gene regulative networks (GRNs) provides an effective tool for hypothesis testing in biology. A necessary step in setting up such models is the estimation of model parameters, i.e., an optimization process during which the difference between model output and given experimental data is minimized. This parameter estimation step is often difficult, especially for larger systems due to often incomplete quantitative data, the large size of the parameter space, and non-linearities in system behavior.

Addressing the task of parameter estimation, we investigate the influence multiobjectivization can have on the optimization process. On the example of an established model for the segment polarity GRN in *Drosophila*, we test different multiobjectivization scenarios compared to a single-objective function proposed earlier for the parameter optimization of the segment polarity network model. Since, instead of a single optimal parameter setting, a set of optimal parameter settings exists for this GRN, the comparison of the different optimization scenarios focuses on the capabilities of the different scenarios to identify optimal parameter settings showing good diversity in the parameter space. By embedding the objective functions in an evolutionary algorithm (EA), we show the superiority of the multiobjective approaches in exploring the model's parameter space.

Categories and Subject Descriptors

J.3.a [**Computer Applications**]: Life and Medical Sciences—Biology and Genetics; I.6.5.a [**Computing Methodologies**]: Simulation, Modeling, and Visualization—Model Development

General Terms

Experimentation

Keywords

Multiobjectivization, parameter estimation

GECCO'09, July 8–12, 2009, Montréal, Québec, Canada.

1. INTRODUCTION

Mathematical modeling of multi-cell/tissue level systems becomes increasingly popular in biology due to the progress of experimental techniques that allows for more and more detailed views on this type of large and complex systems. In this context mathematical models are used on the one hand to validate hypotheses [5, 10, 35] and on the other hand to develop new hypotheses on underlying mechanisms [21, 34]. Although mathematical modeling thereby provides a powerful tool for the investigation of such systems, modeling itself poses some challenges of its own: a major problem involved in modeling is the tuning of model parameters. Especially in scenarios like in the afore mentioned studies, the process of estimating suitable parameters is extremely difficult since system-wide quantitative data is scarcely available—therefore the rich body of methods for parameter estimation [23, 26, 29, 33] relying on detailed quantitative time course data is not applicable.

We here address the task of parameter estimation under mostly qualitative data, i.e., we aim at the identification of parameter settings for which the difference between model output and qualitative experimental results is minimized. In this context, three approaches can be found in the literature: (i) parameters are tuned by hand [21, 35], (ii) the considered models are solved analytically to identify suitable parameters—or at least information about analytical results are used to guide the optimization process [5, 10], (iii) optimization techniques are used to minimize the difference between model output and experimental results [34]. The first two approaches do not allow for testing of new hypotheses on system composition or a rigorous exploration of the parameter space where not only a single fitting parameter setting is sought but different regions of the parameter space containing fitting settings. Moreover tuning by hand and analytical techniques are only feasible for small systems. For larger systems, when aiming at automating the process of parameter estimation or at the exploration of the parameter space, optimization methods are used. Still, the use of optimization techniques introduces new challenges of their own: the definition of suitable objective functions to guide the optimization process.

In this study we investigate different multiobjectivization scenarios [13, 22] and their impact on the parameter optimization process. As example system, we use the segment polarity network model presented in [34], a mid-size to large GRN for *Drosophila*. This model has the advantage that it is well studied and at the same time the parameter estimation process is comparatively easy—a random sampling

approach for parameter space exploration proposed by von Dassow *et al.* [34] already provided good results.

In detail, we test the influence of different decompositions of the proposed single objective function [34] on the optimization of model parameters for the considered example GRN model for the segment polarity network. As optimizations technique we use EAs [2, 9], a class of optimization techniques that already showed good results for other parameter optimization tasks [23, 24]. Since, instead of a single optimal parameter setting, a set of optimal parameter settings exists for the test system, we assess the performance of the tested decompositions with respect to the resulting exploration capabilities: in addition to minimizing the difference between simulated and experimental data, the parameter optimization process should maximize the diversity in the parameter space of the set of found parameter settings.

The paper is organized as follows: in Sec. 2 we briefly describe the segment polarity GRN and formulate the parameter estimation task for the given scenario. In Sec. 3 we present the used EAs as well as the designed objective functions and the implementation of the GRN model. This is followed by simulation results on the chosen approach (Sec. 4) and concluding remarks (Sec. 5).

2. DESCRIPTION OF TEST SYSTEM AND PROBLEM FORMULATION

Here we give a brief introduction to the segment polarity GRN that is used as test scenario in this study, followed by a formal problem description of the considered parameter estimation task.

2.1 Segment Polarity Network

The segment polarity network is a sub-network to the segmentation GRN responsible for body segmentation that plays a crucial role during *Drosophila* development. The formation of the body segments encompasses 3 different groups of genes which are active during different stages. First, information on the location of the anterior/posterior body axis of *Drospohila* is taken up and a first crude division of the body is established by the gap genes. This division is refined to the 14 body segments following the pattern formed by the pair-rule genes. Finally, the polarity of the body segments is defined due to a pattern formed by the segment polarity network.

The segment polarity network uses the pair-rule gene pattern as input stimulus, the segment polarity genes establish an asymmetric, stable patterning for the principle outputs, i.e., the gene product distributions of the genes *wingless* (*wg*), *hedgehog* (*hh*), and *engrailed* (*en*) [34]. The current knowledge on the gene regulative processes between the segment polarity genes is subsumed by a large GRN model by von Dassow *et al.*, made up by a set of 13 differential equations and encompassing nearly 50 free parameters such as rate constants and other kinetic constants, cf. supplementary information of [34] for model details. A sketch of the segment polarity GRN is shown in Fig. 1.

2.2 Problem Formulation

This study aims at testing the impact of multiobjectivization on parameter space exploration of the segment polarity GRN model of *Drosophila*. The considered GRN is a good

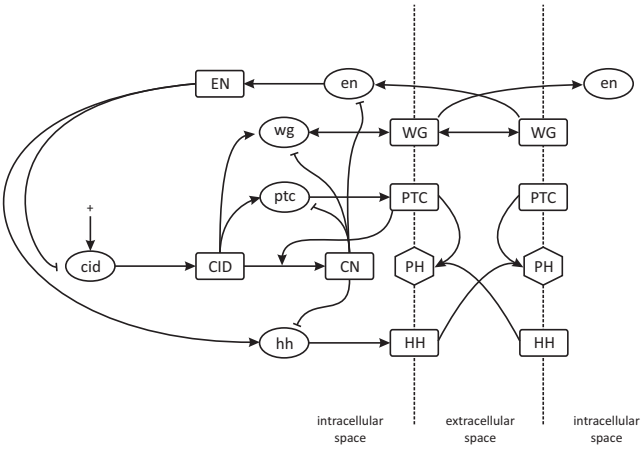

Figure 1: A sketch of the segment polarity GRN (adopted from [34]): ellipses represent mRNAs, rectangles represent proteins, the hexagon represents a protein complex and the '+' represents basal expression. The interactions between the different considered species are given by arrows (positive interactions) and arrow stubs (negative interactions). To reflect the spatial component of the GRN, the interface between two neighboring cells is shown.

example network due to its biological relevance and at the same time being interesting for modeling due to its size while remaining tractable for parameter estimation. In context of parameter space exploration, parameter settings resulting in a patterning of the *Drosophila* body segments as known from experimental studies are to be identified. The target pattern is defined by the spatial distribution of the gene products of 3 segment polarity genes *en*, *wg*, and *hh* which are supposed to form a timely stable and spatially heterogeneous pattern. Since there exists a set of different parameter settings resulting in the desired pattern [34], exploration aims at identifying a representative set of fitting parameter settings, i.e., a set of parameter settings that result in the desired target pattern while being as diverse as possible with respect to the parameter space. This exploration task is formally described by the following expression:

$$\underset{x \in X}{\operatorname{argmin}} \{f(x)\} \tag{1}$$

Where x is a parameter setting in the parameter space $X \subseteq \mathbb{R}^n$ and $f : X \mapsto \mathbb{R}$ is a scoring function measuring the deviation between the desired outcome and the outcome resulting from the parameter setting x. An optimal parameter setting x^{opt} therefore has the minimal score of $f(x^{opt}) = 0$.

Instead of considering the single-objective task, it might be advantageous to decompose the function f into a set of functions $F(x) = (f_1(x), \ldots, f_m(x))$. This multiobjectivization is a straightforward procedure for the given optimization problem: as mentioned before, f already depends on a set of 3 different genes (*en*, *wg*, *hh*) and for each of these on 2 different characteristics (pattern stability, pattern match) allowing to subdivide f in a set of up to 6 different objectives. The advantage of such a decomposition is anticipated to be twofold: first, the multiobjectivization potentially aids the optimization process [7, 11, 12, 13, 19, 22, 25]. Second, we are interested in a set of optimal solutions rather than a

single solution (as usually provided by single-objective methods). Therefore reformulating the task as a multiobjective problem could allow to identify a set of different optimal solutions within a single run and thereby make a more efficient use of the available computation time. The multiobjective problem is formally described by identifying the set:

$$\{x \in X | \nexists\, x' \in X : x' \preceq x \wedge x \npreceq x'\} \quad (2)$$

Where x, x' are parameter settings again in the parameter space $X \subseteq \mathbb{R}^n$ and '$\preceq$' denotes the weak Pareto-dominance relation (cf. Def. 1) with respect to the vector valued function $F(x)$. In other words, Eq. 2 denotes the Pareto-set of the multiobjective optimization problem; the image of the Pareto-set is called the Pareto-front. As mentioned above, the Pareto-front of the considered problem is given by a single point onto which all optimal parameter settings are mapped. On the other hand, the Pareto-set contains several parameter settings and a good approximation of the Pareto-set should contain a sub-set of the Pareto-set that reflects its diversity in parameter space.

DEFINITION 1 (WEAK PARETO-DOMINANCE). *For vector valued functions $F(x) = (f_1(x), \ldots, f_m(x))$ and two vectors $x, x' \in \mathbb{R}^n$, x is said to weakly dominate x' ($x \preceq x'$) iff $x_i \leq x'_i \,\forall\, i \in \{1, \ldots, m\}$.*

3. APPROACH

In this section we describe first the used algorithms, followed by the proposed objective functions, ending with a description of our implementation of the GRN that is used to generate the data necessary for the evaluation of the objectives.

3.1 Algorithms

To contrast the random sampling approach used in [34] and to address the former optimization tasks (cf. Eq. 1 and Eq. 2), we propose the use of evolutionary algorithms (EAs). EAs have been used in a range of studies for parameter optimization [17, 23, 24, 28]. We decided to use the Covariance Matrix Adaption Evolution Strategy (CMA-ES) developed by Hansen and Ostermeier [15] and its multiobjective variant [18] for this study. Both algorithms have proven their qualities in real coded optimization on a range of applications [24, 27] as well as theoretical studies [1, 14, 18].

While in the single-objective case we use the standard CMA-ES (version 3.24 beta), we introduce a slight variation to the the multiobjective CMA-ES (MO-CMA-ES): instead of the exact hypervolume indicator [36], for the environmental selection step we approximate the hypervolume using a method based on Monte Carlo sampling, HypE [3]. This change is introduced since the computation of the hypervolume is shown to be $\#\mathcal{P}$-hard [6] and the fastest known algorithm has a run time complexity of $\mathcal{O}(p^{\frac{m}{2}})$ [4] (with p the number of individuals and m the number of objectives). In consequence, computation of the exact hypervolume indicator is practically infeasible already for settings with 5 objectives and about 50 individuals—a scenario we have to consider since we use more than 5 objectives.

3.2 Objective Function

As discussed in the supplementary information of [34], a single-objective function can be used for the optimization of model parameters: it encompasses elements scoring pattern match of the gene product distributions of the three genes *en*, *wg*, *hh* as well as the stability scores for the simulated time of the pattern defined by the 3 genes. In other words, this fitness function is a weighted sum of stability measures and pattern match scores—objective components we explain in detail in the following.

This composition of different components allows for a quite straightforward decomposition by considering the single components as own objectives—a route we follow for our multiobjectivization approach. In addition, we propose an objective explicitly measuring the diversity of the parameter settings in the parameter space. We deem this to be a plausible addition since the task of parameter estimation of the considered GRN explicitly encompasses maximizing the diversity of the found optimal parameter settings with respect to the parameter space.

3.2.1 Pattern Scoring

Following the suggestion of von Dassow *et al.* (supplementary information to [34]) we evaluate the forming pattern by comparing the simulation output to a mask defining the target pattern $p_{tar} = \{on, off\}^{|C|}$ (with C being the set of cells forming the considered domain and $|C|$ being its cardinality), indicating which genes are active in which cell. To assess the match between simulated pattern and target pattern the simulated data is discretized. For this descretization we use the proposed threshold of $\delta_t = 0.1$: whenever a concentration $[c_i] \geq \delta_t$ $(i = 1, \ldots, |C|)$ the corresponding gene is considered to be active in cell i, resulting in another mask $p_{sim} = \{on, off\}^{|C|}$. The pattern score $f_{pattern}$ then is a discrete function counting the per-cell difference in the simulated pattern and the target pattern for a gene. It is given by the following equation:

$$f_{pattern}(p_{tar}, p_{sim}) = \sum_{i=1,\ldots,|C|} \mathbf{I}(p_{tar,i}, p_{sim,i}) \quad (3)$$

Where $\mathbf{I}(p_{tar,i}, p_{sim,i})$ is an indicator function which becomes 1 iff $p_{tar,i}$ XOR $p_{sim,i} = true$ for cell i in the masks and 0 otherwise.

3.2.2 Stability Scoring

To assess the stability of the resulting patterns, we chose a different approach than von Dassow *et al.*; they used a sliding window on the time-course data of their simulations in order to detect oscillations admitting that the oscillation detection was their main reason for false scoring of patterns (personal communication). Nevertheless, the number of false decisions was rather small. Here we propose to use a criterion based on Fourier analysis, the spectral envelope [31, 32]. The spectral envelope provides a way to map the variance in a time-series signal to a set of frequency indexed oscillating components (sines and cosines). The spectral envelope then gives a measure to which proportion the variance in the signal can be attributed to a certain oscillating component. Here we chose the implementation of the spectral envelope method proposed in [20]: The time series data $\mathcal{X}'_t$ of all cells with respect to a single gene is considered. It is given as a matrix where the concentrations of the cells are ordered in rows and the columns represent the time course for the time points $t = 1, \ldots, k$. The data is first mean-centered and made unit variant. Using the normalized data $\mathcal{X}$, we approximate the frequency discretized periodogram

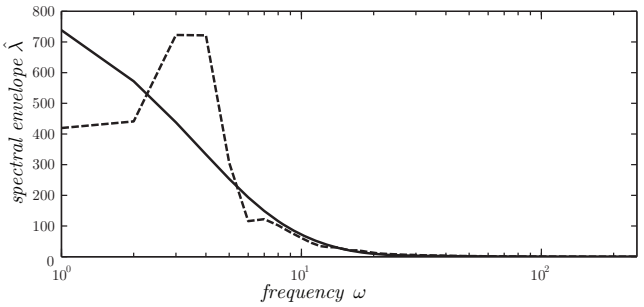

Figure 2: Spectral envelopes generated from simulation data for the segment polarity GRN model. The solid line shows the envelope for a typical stable time course of the gene *hh* while the dashed line shows the envelope for an oscillating time course for the same gene.

$\hat{I}_k(\omega)$ as:

$$\hat{I}_k(\omega_j) = \left| \frac{1}{k} \left[\sum_{t=0}^{k-1} x(t)\ \exp(-2\pi i \omega_j t) \right] \cdot \left[\sum_{t=0}^{k-1} x(t)\ \exp(-2\pi i \omega_j t) \right]^* \right| \quad (4)$$

Where the frequencies $\omega_j = \frac{j}{k}, j = 1, \ldots, \lfloor \frac{k}{2} \rfloor$ are considered, $x(t)$ denotes the concentrations in all cells at time t, $i^2 = -1$, and '*' denotes the conjugate transpose. The resulting periodogram is smoothed using a sliding window with respect to the frequencies:

$$\hat{P}_{\mathcal{X}}(\omega_j) = \frac{1}{4}\hat{I}_k(\omega_{j-1}) + \frac{1}{2}\hat{I}_k(\omega_j) + \frac{1}{4}\hat{I}_k(\omega_{j+1}) \quad (5)$$

The spectral envelope $\hat{\lambda}(\omega_j)$ can then be estimated by taking the largest eigenvalues of $\hat{P}_{\mathcal{X}}(\omega_j)$ iterating over all frequencies ω_j. For details on the derivation see [20, 32].

Given a noisy signal containing an oscillation, the spectral envelope shows a peak for the frequencies explaining the most variance in the original signal. For a signal that is flat apart from the oscillation the peak should be narrow (cf. Fig. 4 in [20]). Since the simulation data we gather by numerical integration of the differential equation model is noise-free and since the simulations include a transient part where concentrations vary strongly, we need to take a slightly different approach to identify oscillations in the spectral envelope. In a typical spectral envelope of the simulated data (see Fig. 2), we observe a bulge for the lower frequencies that is quasi-monotonically decreasing with growing frequencies. Now we deem a time course as oscillating as soon as the envelope $\hat{\lambda}(\omega)$ is getting larger by at least $\delta_{osc} = 10^{-3}$ for increasing frequencies ω. The oscillation score f_{osc} is computed using Eq. 6. It has to be minimized and has its optimum at $f_{osc} = 0$. The used δ_{osc} has been determined experimentally and the criterion itself was tested on a set of sample time courses from the segment polarity GRN model.

$$f_{osc}(\hat{\lambda}) = \max_{j=2,\ldots,\lfloor \frac{k}{2} \rfloor} \left\{ \left| \min \left\{ \hat{\lambda}(\omega_{j-1}) - \hat{\lambda}(\omega_j) + \delta_{osc}, 0 \right\} \right| \right\} \quad (6)$$

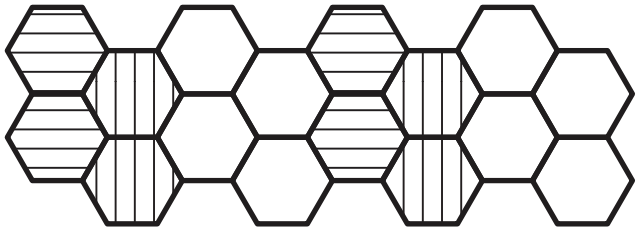

Figure 3: Schematic view on the simulated cell domain showing the pre-pattern used as initial condition to the numerical integration: in cells hatched with horizontal lines *wg* levels and those of the encoded protein are set to 1 while in cells hatched with vertical lines *en* levels and those of the encoded protein are set to 1. For all other genes and cells the initial concentrations are set to 0.

3.2.3 Diversity Scoring

In order to assess decision space diversity we propose the following criterion: we determine a ranking on a given set of parameter vectors $\{x^1, \ldots, x^k\} \in X$ with $X \subseteq \mathbb{R}^n$ being the n dimensional parameter space. The ranking is build using a Monte Carlo procedure: we draw uniformly distributed sample parameter vectors $\{s^1, \ldots, s^j\} \in X$ and for each of the sampled vectors s^h $(h = 1, \ldots, j)$ we compute its Euclidean distance to all parameter vectors x^i $(i = 1, \ldots, k)$. For each of the j sample vectors we then generate a ranking on the x^i were the best rank $r = 1$ is assigned to the x^i with the minimal distance to s^h. The worst rank $r = k$ is assigned to the parameter vector x^i with the maximal Euclidean distance to s^h. After all sample rankings have been built the final rankings are determined: for each vector x^i all its j rankings are summed up and the final ranking is given by the ascending order on the summed ranks for every x^i.

As number of samples to be drawn for the final ranking we chose $j = 3810$—following Hoeffding's inequality [16] using 3810 samples results in a probability of 0.90 of resulting in an error in coverage computation of $err \leq 0.125$. For this calculation we approximated the expected distance of two parameter settings in the parameter space $X = [0, 1]^{49}$ with the worstcase distance of 7.

3.3 Model Implementation

We re-implemented the model described in the supplementary information of [34] in MATLAB®. In agreement with the presented model, as simulated domain we use 2 rows of 8 hexagonal cells (see Fig. 3). The cells are connected with each other via adjacent cell faces allowing for cell-cell communication by exchange of gene products. Like von Dassow *et al.* we assume periodic boundary conditions for the simulated domain. Simulations of the GRN are conducted by numerical integration of the 13 differential equations composing the model. For the numerical integration of the resulting system we use an implicit-explicit scheme consisting of a modified Crank-Nicolson scheme and an Adam-Bashford scheme [30] with a time step $\Delta_t = 0.2$ min and a spatial discretization in cellular resolution. As simulated time interval we chose a window of 1000 min like in [34].

As initial conditions for the numerical simulation we use the same conditions as proposed by von Dassow *et al.*: all

Table 1: Details for the hypervolume calculations: for each of the considered MO-CMA-ES setups (using from 2 to 7 objectives) the reference points and the ordering of the objectives are given. Here 'aggr. score' is an aggregated score for stability and pattern match for a given set of genes, 'stab. score' is the stability score for a single gene, 'pattern score' is the pattern match score for a single gene, and 'div. score' is the diversity score for a set of parameter vectors.

Optimizer	Reference point	Objective order
CMA-ES	–	aggr. score over all genes
MO 2 obj.	(1260, 1.5)	aggr. score over all genes, div. score
MO 3 obj.	(420, 420, 420)	aggr. score separately for *en*, *wg*, *hh*
MO 4 obj.	(420, 420, 420, 1.5)	aggr. score separately for *en*, *wg*, *hh*, div. score
MO 6 obj.	(400, 400, 400, 20, 20, 20)	stab. score for *en*, *wg*, *hh*, pattern score for *en*, *wg*, *hh*
MO 7 obj.	(400, 400, 400, 20, 20, 20, 1.5)	stab. score for *en*, *wg*, *hh*, pattern score for *en*, *wg*, *hh*, div. score

concentrations for all genes are set to 0 except for the RNA and the thereby encoded protein of *en* in the cells of the 2^{nd} and 6^{th} column as well as those of *wg* in the cells of the 1^{st} and 5^{th} column. In these cells the concentrations are set to 1. Additionally, the basal expression level for the RNA of *cid* in Eq. h (supplementary information of [34]) is set to 0.4. The resulting pre-pattern for *en* and *wg* is shown in Fig. 3.

4. SIMULATIONS AND RESULTS

In this section we first describe the performance metrics with which we evaluate our multiobjectivization approach, followed by a description of the simulation setup, and finally presenting results for the simulation runs.

4.1 Performance Metrics

In order to evaluate the proposed approaches we compare the evolutionary approaches to random sampling (as reported in [34]). The comparison is done with respect to 2 different performance indicators: (i) the mean number of distinct optima found within 3000 evaluations, (ii) the mean inverse coverage of the parameter space achieved within 3000 evaluations. Whereas the first metric is straightforward, we would like to give a brief explanation how we asses the inverse coverage: for a set of optimal parameter vectors $x^i \in \{x^1, \ldots, x^k\}$ the inverse coverage is given by the expected minimal distance of any of the vectors x^i to any random vector in the parameter space X. We approximate the expected value of the minimal distance again using Monte Carlo sampling. We generate a set of sample vectors $s^h \in \{s^1, \ldots, s^j\}$ and calculate for each of the s^h the minimal Euclidean distance to the x^i. The average of these j minimal distances is used as approximation of the inverse coverage. We use 381000 samples for this approximation which using Hoefding's inequality [16] results in a probability of 0.90 of resulting in an approximation error $err \leq 0.0125$. In Hoefding's inequality, we approximate the expected distance of vectors in the parameter space $X = [0, 1]^{49}$ with its worstcase distance of 7.

4.2 Simulation Setup

While for random sampling we take the reported value of in average 1 hit per 200 samples in identifying an optimal parameter setting, we determined the values experimentally for CMA-ES and the different MO-CMA-ES. For the single-objective CMA-ES we use the standard parameters except the following: maximal number of evaluations of 3000, population size of 30, target fitness of 10^{-8}. Additionally we used a restart strategy: after termination and as long as there are evaluations left, the CMA-ES is restarted with a new initial vector and the same parameters. For the multi-objective MO-CMA-ES we use 5 different sets of objective functions: (i) using the diversity function (see Sec. 3.2.3) and the objective function used for the single-objective case: aggregating stability scores (see Sec. 3.2.2) and pattern scores (see Sec. 3.2.1) for all genes; (ii) aggregating stability score and pattern score for each gene resulting in 3 objective functions (iii) using the 3 afore mentioned objective function plus the diversity function; (iv) using stability score and pattern score separately for each gene resulting in 6 objective functions; (v) using the 6 afore mentioned objective function plus the diversity function. For the MO-CMA-ES we used a population size of 100 and allowed again 3000 evaluations per run. For the HypE procedure we used 10000 samples and reference points as shown in Tab. 1. For CMA-ES and MO-CMA-ES with the 5 different objective function sets we did 21 runs each where every run took approximately a day on a two chip dual core AMD Opteron $2.6GHz$ 64-bit machine with $8GB$ RAM using MATLAB® 7.6 (R2008a).

4.3 Results and Discussion

The reported hit rate for random sampling results on average in 15 optimal parameter settings found in 3000 evaluations, the CMA-ES found on average about 6 optimal parameter settings in 3000 evaluations, and the MO-CMA-ES found on average more than 25 different optimal parameter settings for any of the considered set of objectives (see Tab. 2). The fact that random sampling produces better results than the CMA-ES is surprising on the first glance but has to be relativized: the considered parameter optimization task is comparably easy which is documented by the fact that random sampling is that successful. For the CMA-ES this fact results in a problem since the optimization process would need to converge within 7 generations in order to keep up with random sampling—random sampling identifies an optimum every 200 samples which compares to 7 generation with 30 evaluations per generation for the CMA-ES. To demonstrate its full potential, the CMA-ES would need a more difficult task. Nevertheless, the MO-CMA-ES in average found more than 25 optimal parameter settings clearly improving the results of both, CMA-ES and random sampling. This can be seen as strong indicator for the effectiveness of the multiobjectivization approach and the feasibility of applying EAs like the MO-CMA-ES to the considered optimization task in the first place. The supe-

Table 2: Results for sampling, CMA-ES, and MO-CMA-ES runs: for all considered combinations of objectives the mean number of found optima (∅(# opt)) and the mean inverse coverage values (∅(inv cov)) are given, except for the sampling approach: for sampling only the mean number of found optimal parameter settings is given which is calculated based on information given in [34]. In addition, for each considered scenario the number of significantly better (following Conover-Inman) scenarios are given for the coverage values (rank cov) and the numbers of found optima (rank opt) as well as the coverage values (cov) and numbers of optimal solutions (# opt) for all 21 runs.

	Sampling	CMA-ES	MO 2 obj.	MO 3 obj.	MO 4 obj.	MO 6 obj.	MO 7 obj.
∅(# opt)	15	6.5714	28.3333	25.5714	25.3810	28.3333	26.6190
∅(inv cov)	–	0.3634	0.3422	0.3456	0.3442	0.3431	0.3451
rank opt	5	6	0	0	0	0	0
rank cov	–	5	0	0	0	0	0

	cov	# opt	cov	# opt	cov	# opt	cov	# opt	cov	# opt	cov	# opt
run 1	0.385	3	0.349	28	0.349	31	0.340	23	0.335	31	0.342	26
run 2	0.367	5	0.345	17	0.356	16	0.339	34	0.344	27	0.351	20
run 3	0.353	10	0.336	30	0.350	18	0.345	25	0.338	22	0.344	32
run 4	0.360	8	0.338	41	0.348	20	0.357	16	0.337	29	0.344	34
run 5	0.362	6	0.346	21	0.340	43	0.347	25	0.346	16	0.346	22
run 6	0.369	6	0.341	34	0.336	49	0.347	33	0.341	30	0.344	28
run 7	0.357	8	0.346	33	0.335	26	0.338	32	0.347	18	0.355	16
run 8	0.360	8	0.350	24	0.356	16	0.345	18	0.342	24	0.344	45
run 9	0.365	6	0.341	26	0.342	31	0.345	28	0.345	31	0.333	41
run 10	0.361	7	0.340	30	0.337	38	0.344	20	0.344	41	0.337	24
run 11	0.359	7	0.344	32	0.350	12	0.345	28	0.344	18	0.341	38
run 12	0.352	7	0.343	28	0.338	38	0.344	17	0.341	22	0.337	31
run 13	0.363	7	0.340	25	0.351	19	0.352	16	0.342	28	0.352	28
run 14	0.377	5	0.339	35	0.332	39	0.339	29	0.357	14	0.348	22
run 15	0.365	6	0.343	23	0.351	25	0.349	17	0.346	23	0.341	22
run 16	0.370	6	0.340	32	0.344	19	0.338	32	0.334	57	0.351	13
run 17	0.361	7	0.348	18	0.343	34	0.342	31	0.339	43	0.346	22
run 18	0.351	7	0.334	36	0.358	22	0.337	39	0.335	34	0.348	25
run 19	0.368	6	0.339	33	0.352	10	0.348	19	0.360	13	0.336	43
run 20	0.370	6	0.341	29	0.351	17	0.343	16	0.343	36	0.345	15
run 21	0.360	7	0.343	20	0.341	14	0.346	35	0.346	28	0.362	12

riority of the MO-CMA-ES is documented by the inverse coverage measure as well: all tested MO-CMA-ES variants improve the inverse coverage compared to the CMA-ES by about 5% (see Tab. 2). We tested these results for statistical significance, first using the Kruskal-Wallis test [8] at a significance level of $\alpha = 0.05$. We were able to reject the H_0 hypothesis that there is no significant difference in median with respect to number of found optima and coverage between the multiobjective scenarios, the single objective CMA-ES and random sampling. Thereafter, for all pairs of algorithms the difference in the number of found optima and coverage values is compared using the Conover-Inman procedure [8] with the same α level as in the Kruskal-Wallis test . In result the statistical testing shows that the multiobejctivization strategies are significantly better than both, single objective CMA-ES and random sampling, random sampling is significantly better than the single objective CMA-ES, and there is no significant difference between the different multiobjective scenarios. Surprising about this result is that there is no clear difference between the different multiobjectivization setups. At least between those multiobjective variants using the diversity criterion and those only using stability and pattern match we would have expected a difference: while stability and pattern match define the original criteria for the optimization, decision space diversity is completely unrelated and including it in the optimization process should result in a restructuring of the fitness landscape. We would have expected that this restructuring causes an effect visible in the results. The fact that the results do not reflect this in part might again stem from the fact that the parameter optimization task for the considered network is comparably easy but as well could be an inherent property of the considered GRN or the considered target pattern.

5. CONCLUSIONS

In the present study we investigated the impact of multiobjectivizations strategies on the exploration of parameter spaces of GRN models. As a test case we used an established GRN model for the segment polarity network in *Drosophila* and tested a set of decompositions and extensions to the originally proposed objective function for the respective parameter optimization. We embedded the objective functions in standard evolutionary algorithms and compared the results with respect to the number of found optimal parameter settings and their resulting coverage of the parameter space. It turned out that all tested multiobjective variants were superior to the original single objective criterion in terms of both metrics thereby documenting the feasibility of multiobjectivization for the given task of parameter exploration on the GRN model.

Notably there was no difference between the results using the different multiobjective setups; probably due to the fact that the parameter estimation on the chosen test system is comparatively easy or due to the possibility that apart from the pattern formed by the 3 genes *en*, *wg*, and *hh*, the target behavior is defined by the exact behavior of other genes or gene products as well. In consequence the considered parameter optimization task would be under-determined and could yield some false positive parameter settings. In the following we plan to apply the proposed approach to more demanding GRN models for otherwise comparable systems like they can be found in *Arabidopsis* meristems.

6. REFERENCES

[1] A. Auger and N. Hansen. Performance evaluation of an advanced local search evolutionary algorithm. In *Congress on Evolutionary Computation (CEC 2005)*, volume 2, pages 1777–1784, Piscataway, NJ, USA, 2005. IEEE Press.

[2] T. Bäck, D. B. Fogel, and Z. Michalewicz, editors. *Handbook of Evolutionary Computation*. IOP Publishing and Oxford University Press, Bristol, UK, 1997.

[3] J. Bader and E. Zitzler. HypE: An Algorithm for Fast Hypervolume-Based Many-Objective Optimization. TIK Report 286, Computer Engineering and Networks Laboratory (TIK), ETH Zurich, Nov. 2008.

[4] N. Beume and G. Rudolph. Faster S-Metric Calculation by Considering Dominated Hypervolume as Klee's Measure Problem. Technical Report CI-216/06, Sonderforschungsbereich 531 Computational Intelligence, Universität Dortmund, 2006.

[5] D. Bouyer, F. Geier, F. Kragler, A. Schnittger, M. Pesch, K. Wester, R. Balkunde, J. Timmer, C. Fleck, and M. Hülskamp. Two-Dimensional Patterning by a Trapping/Depletion Mechanism: The Role of TTG1 and GL3 in Arabidopsis Trichome Formation. *PLoS Biol*, 6(6):e141, 2008.

[6] K. Bringmann and T. Friedrich. Approximating the Volume of Unions and Intersections of High-Dimensional Geometric Objects. In S. H. Hong, H. Nagamochi, and T. Fukunaga, editors, *International Symposium on Algorithms and Computation (ISAAC 2008)*, volume 5369 of *LNCS*, pages 436–447, Berlin, Germany, 2008. Springer.

[7] D. Brockhoff, T. Friedrich, N. Hebbinghaus, C. Klein, F. Neumann, and E. Zitzler. Do Additional Objectives Make a Problem Harder? In D. Thierens et al., editors, *Genetic and Evolutionary Computation Conference (GECCO 2007)*, pages 765–772, New York, NY, USA, 2007. ACM Press.

[8] W. J. Conover. *Practical Nonparametric Statistics*. John Wiley, 3 edition, 1999.

[9] K. Deb. *Multi-Objective Optimization Using Evolutionary Algorithms*. Wiley, Chichester, UK, 2001.

[10] F. Geier, J. U. Lohmann, M. Gerstung, A. T. Maier, J. Timmer, and C. Fleck. A Quantitative and Dynamic Model for Plant Cell Regulation. *PLoS ONE*, 3(10):e3553, 2008.

[11] J. Handl and J. Knowles. An Evolutionary Approach to Multiobjective Clustering. *IEEE Transactions on Evolutionary Computation*, 11(1):56–76, 2007.

[12] J. Handl, S. C. Lovell, and J. Knowles. Investigations into the Effect of Multiobjectivization in Protein Structure Prediction. In G. Rudolph et al., editors, *Conference on Parallel Problem Solving From Nature (PPSN X)*, volume 5199 of *LNCS*, pages 702–711. Springer, 2008.

[13] J. Handl, S. C. Lovell, and J. Knowles. Multiobjectivization by Decomposition of Scalar Cost Functions. In G. Rudolph et al., editors, *Conference on Parallel Problem Solving From Nature (PPSN X)*, volume 5199 of *LNCS*, pages 31–40. Springer, 2008.

[14] N. Hansen and S. Kern. Evaluating the CMA

Evolution Strategy on Multimodal Test Functions. In X. Yao et al., editors, *Conference on Parallel Problem Solving from Nature (PPSN VIII)*, volume 3242 of *LNCS*, pages 282–291, Berlin, Germany, 2004. Springer.

[15] N. Hansen and A. Ostermeier. Adapting arbitrary normal mutation distributions in evolution strategies: the covariance matrix adaptation. In *Congress on Evolutionary Computation (CEC 1996)*, pages 312–317, Piscataway, NJ, USA, 1996. IEEE.

[16] W. Hoeffding. Probability Inequalities for Sums of Bounded Random Variables. *Journal of the American Statistical Association*, 58(301):13–30, 1963.

[17] T. Hohm and E. Zitzler. Modeling the Shoot Apical Meristem in A. thaliana: Parameter Estimation for Spatial Pattern Formation. In E. Marchiori, J. H. Moore, and J. C. Rajapakse, editors, *Evolutionary Computation, Machine Learning and Data Mining in Bioinformatics*, volume 4447 of *LNCS*, pages 102–113. Springer, 2007.

[18] C. Igel, N. Hansen, and S. Roth. Covariance Matrix Adaptation for Multi-objective Optimization. *Evolutionary Computation*, 15(1):1–28, 2007.

[19] M. T. Jensen. Helper-Objectives: Using Multi-Objective Evolutionary Algorithms for Single-Objective Optimisation. *Journal of Mathematical Modelling and Algorithms*, 3(4):323–347, 2004.

[20] H. J. Jiang, M. A. A. S. Choudhury, and S. L. Shah. Detection and diagnosis of plant-wide oscillations from industrial data using the spectral envelope method. *J Process Contr*, 17:143–155, 2007.

[21] H. Jönsson, M. Heisler, G. V. Reddy, V. Agrawal, V. Gor, B. E. Shapiro, E. Mjolsness, and E. M. Meyerowitz. Modeling the organization of the WUSCHEL expression domain in the shoot apical meristem. *Bioinformatics*, 21:i232–i240, 2005.

[22] J. D. Knowles, R. A. Watson, and D. W. Corne. Reducing Local Optima in Single-Objective Problems by Multi-objectivization. In E. Zitzler et al., editors, *Conference on Evolutionary Multi-Criterion Optimization (EMO 2001)*, volume 1993 of *LNCS*, pages 269–283, Berlin, 2001. Springer.

[23] P. Mendes and D. B. Kell. Non-linear optimization of biochemical pathways: applications to metabolic engineering and parameter estimation. *Bioinformatics*, 14(10):869–883, 1998.

[24] C. G. Moles, P. Mendes, and J. R. Banga. Parameter Estimation in Biochemical Pathways: A Comparison of Global Optimization Methods. *Genome Research*, 13(11):2467–2474, 2003.

[25] F. Neumann and I. Wegener. Minimum Spanning Trees Made Easier Via Multi-Objective Optimization. *Natural Computing*, 5(3):305–319, 2006. Conference version in Beyer et al. (Eds.): Genetic and Evolutionary Computation Conference - GECCO 2005, Volume 1, ACM Press, New York, USA, pages 763–770.

[26] P. K. Polisetty, E. O. Voit, and E. P. Gatzke. Identification of metabolic system parameters using global optimization methods. *Theoretical Biology and Medical Modelling*, 3(4), 2006.

[27] R. Quast, R. Baade, and D. Reimers. Evolution Strategies applied to the problem of line profile decomposition in QSO spectra. *Astron Astrophys*, 431:1167–1175, 2005.

[28] B. J. Reardon. Optimization of densification modelling parameters of beryllium powder using a fuzzy logic based multiobjective genetic algorithm. *Modelling Simul. Mater. Sci. Eng.*, 6:735–746, 1998.

[29] M. Rodriguez-Fernandez, J. A. Egea, and J. R. Banga. Novel metaheuristics for parameter estimation in nonlinear dynamical biological systems. *BMC Bioinformatics*, 7(483), 2006.

[30] S. J. Ruuth. Implicit-explicit methods for reaction-diffusion problems in pattern formation. *J Math Biol*, 34(2):148–176, 1995.

[31] D. S. Stoffer, D. E. Tyler, and A. J. McDougall. Spectral analysis for categorical time series: Scaling and the spectral envelope. *Biometrika*, 80(3):611—622, 1993.

[32] D. S. Stoffer, D. E. Tyler, and D. A. Wendt. The Spectral Envelope and Its Applications. *Stat Sci*, 15(3):224—253, 2000.

[33] E. O. Voit. *Computational Analysis of Biochemical Systems*. Cambridge University Press, Cambridge, UK, 2000.

[34] G. von Dassow, E. Meir, E. M. Munro, and G. M. Odell. The segment polarity network is a robust developmental module. *Nature*, 406:188–192, 2000.

[35] M. Yamaguchi, E. Yoshimoto, and S. Kondo. Pattern regulation in the stripe of zebrafish suggests an underlying dynamic and autonomous mechanism. *Proc Natl Acad Sci USA*, 104(12):4790–4793, 2007.

[36] E. Zitzler and L. Thiele. Multiobjective Optimization Using Evolutionary Algorithms - A Comparative Case Study. In *Conference on Parallel Problem Solving from Nature (PPSN V)*, pages 292–301, Amsterdam, 1998.